T.1: Bose-Einstein condensation in a dilute atomic gas

S. R. Mishra (srm@cat.ernet.in), S. P. Ram, and S. K. Tiwari

1. Introduction

Since the first observation of Bose-Einstein condensation (BEC) in a dilute atomic gas of ^{87}Rb at JILA (Colourado, USA) in 1995 [1], the research in this field has exploded in several directions and is providing deeper insight in atomic physics, coherent matter waves, atom optics, many-body physics, ultra-cold collisions, degenerate fermions etc. Besides the basic research, the implications to future devices such as atom laser, atom-gyroscope, precision measurements etc. have also received a considerable thrust.

In Laser Physics Applications Division at RRCAT, we have developed a set-up for achieving BEC of ^{87}Rb atoms to learn the technology as well as to explore its applications such as an Atom Laser. The work is at an advanced stage. In this article, we discuss briefly about the process of Bose-Einstein condensation, and then describe some details of our experimental set-up such as the experimental scheme, milestones achieved, and direction and efforts in progress to complete the remaining task.

2. Bose-Einstein Condensation

Though the experiments in 1995 on alkali atoms should be considered as a milestone in the history of BEC [1,2], the experimental and theoretical research on this unique phenomenon predicted by Einstein (1924, 1925) using Bose statistics (1924) for particles with integer spin has attracted attention of researchers for a long time. In particular, super-fluidity in helium was considered by London (1938) as a possible manifestation of BEC. Similarly, narrow line-width emission observed from excitons in semiconductors has also been attributed to BEC of excitons in the ground state. A striking difference between BEC observed in 1995 in samples of dilute atomic gases and that in others is due to weak interactions in dilute atomic gases. The BEC thus observed in these gases can be considered as a purely quantum statistical process as predicted by theory of Bose and Einstein. Since the first observation of BEC in an alkali vapour sample (^{87}Rb) in 1995 at JILA, many groups have succeeded in achieving BEC in atomic gases of different elements such as ^{23}Na, ^{7}Li, ^{85}Rb, ^{41}K, H, He, ^{133}Cs, Cr along with BEC-BCS transitions in fermionic systems of ^{6}Li, ^{40}K, and Yb.

In a sample of indistinguishable particles having integer spin, i.e. bosons, BEC occurs when thermal de Broglie wavelength ($=h/(2\pi mkT)^{1/2}$) becomes comparable to the inter-particle separation. This essentially requires that temperature should be so low that kinetic motion diminishes to the extent that all particles are in the ground state of the system. Mathematically, it is expressed in terms of phase-space density as $n\lambda^3>2.61$, where 'n' is number density of bosons. The phenomenon of BEC is a purely quantum statistical effect, and is specific to the indistinguishability and bosonic nature of the particles under consideration. In real systems such as a gas of atoms, because of finite interactions, observation of BEC is difficult due to requirement of very low temperature (typically T~100-500 nK at density $n\sim10^{13}$-10^{14} cm^{-3} for ^{87}Rb) to reach the above phase-space density condition. Increasing density for sake of a higher temperature, the condensed phase (i.e. solid or liquid) is reached before the BEC phase due to increase in the interaction energy.

With the advent of cooling of atoms using lasers, the path to reach BEC has become much easier than before. Using a laser cooling set-up known as magneto-optical trap (MOT), it is possible to reach temperature typically as low as ~1-10μK in a gas of atoms. Beyond this value, the temperature is lowered by evaporative cooling. In majority cases, to achieve BEC in dilute atomic gases, atoms are initially trapped and cooled in a MOT and then subjected to evaporative cooling in a trap to reach BEC transition. During the evaporation, atoms are trapped either in a magnetic trap formed by an inhomogeneous magnetic field or in a dipole force trap formed by a non-resonant laser beam. To avoid loss of atoms from the trap due to background collisions, evaporative cooling is performed in a UHV chamber at pressure of ~10^{-10} to 10^{-11} Torr. In a magnetic trap, evaporation of atoms is forced by an appropriately designed radio-frequency (RF) field which flips the spin of higher energy atoms selectively and ejects them from the trap. In an optical dipole trap on the other hand, evaporation is executed by lowering the intensity of the trapping laser. Both these methods involve considerable complexity and require an expertise in different areas of physics and engineering.

Since formation of a MOT from vapour needs a larger pressure (~10^{-8} Torr) than that is required in the evaporation chamber (~10^{-10}-10^{-11} Torr), double-MOT systems are built in which atoms are first trapped in a MOT in the vapour chamber and then transferred using a push laser beam to another MOT in a UHV chamber to perform evaporative cooling [3]. Alternatively, now a days, single MOT based BEC systems are also becoming popular, in which a MOT is formed directly in a UHV chamber from the jet of atoms using a Zeeman slower [4]. The Zeeman slower however involves a complex design of magnetic field used in it.

3. BEC set-up at RRCAT

At RRCAT, we have chosen to build a double-MOT system to achieve BEC of ^{87}Rb atoms. A schematic of the system is shown in Fig.T.1.1. In the following we present the details of design, operation of the system and its present status.

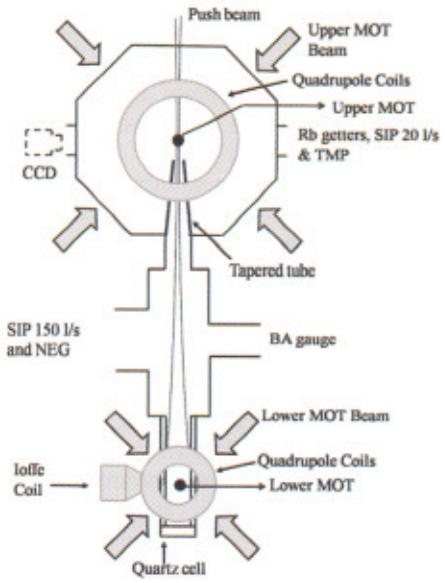

Fig.T.1.1: A schematic of double-MOT set-up developed in our laboratory at RRCAT for BEC of ^{87}Rb atoms.

3.1. Vacuum System

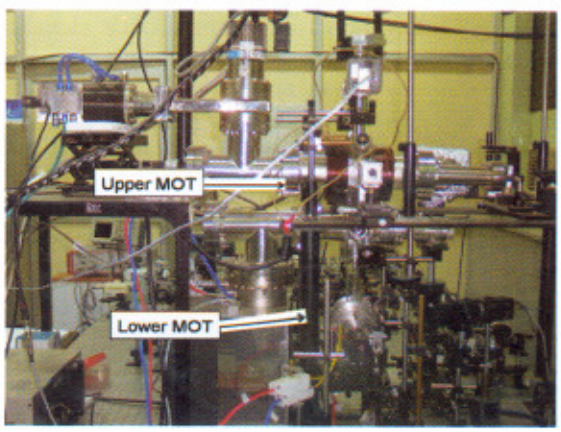

Fig.T.1.2. A photograph of the set-up for BEC.

In our set-up (see photograph in Fig.T.1.2), the vacuum system consists of two parts (upper part and lower part) having different vacuum levels. The upper part is an octagonal chamber of stainless steel (SS) in which upper MOT is formed from the background Rb-vapour at pressure of 2×10^{-8} Torr. The lower part is connected to the upper octagonal chamber by a differential pumping tube which is tapered in shape with inner diameters of 5.0 mm and 12.0 mm at ends and length 70 mm. A chamber in the lower part has connections to a combination pump (a 150 L/s SIP and a NEG module), BA gauge, tapered tube and 25x25x75 mm dimension quartz glass cell (Optiglass, UK). The lower MOT is formed inside this cell after atoms are pushed to the cell from the upper MOT by a push beam. The vacuum chamber was fabricated in Workshop-B of RRCAT.

We use a 70 L/s turbo-molecular pump (TMP) for roughing of the whole vacuum system. A gate-valve is used between the pump and the chamber to isolate the vacuum system from the atmosphere when TMP is off. We have also connected a 20 L/s sputter ion pump for pumping the upper octagonal chamber, in addition to combination pump used in the lower part. The roughing of the vacuum system using TMP was done in presence of mild baking at temperature of 100-150 °C for a prolonged time. Then, at base pressure of 10^{-6} Torr in the system, both the ion pumps were switched-on. After removal of degassing from ion pumps, the gate-valve was closed and TMP was switched-off. With both the ion pumps on, we achieve a pressure of 1×10^{-8} Torr in the upper chamber and 1.2×10^{-9} Torr in the lower chamber without operating the NEG module. When we activated NEG module for about 20 minutes, the vacuum got improved to $\sim1\times10^{-10}$ Torr in the lower chamber.

3.2. Operation of Double-MOT system

In our system, upper MOT is formed in the octagonal chamber having Rb-vapour in the background, and lower MOT is formed in the quartz cell. The upper MOT and lower MOT positions are vertically separated by ~340 mm. For the formation of upper MOT, the Rb-vapour was generated from a getter source (Varian, Italy) which was inserted in the chamber after fixing it on a two-pin feed-through. A DC current of ~3.6 A was supplied to the getter to generate Rb-vapour. With Rb-vapour, the pressure of the upper chamber changes from 1×10^{-8} Torr to 2×10^{-8} Torr.

The cooling laser beams for the upper and the lower MOTs were obtained from two separate grating controlled external-cavity diode lasers (DL-100, TOPTICA, Germany), whereas re-pumping laser beams were obtained by dividing output from a single laser of similar configuration (SACHER, Germany). For each MOT, cooling beam and re-pumping beam were first mixed, and combined beam was then expanded and split into three MOT beams (MB) which entered the chamber. After retro-reflection of each of these three beams from a mirror at exit of the chamber, required six MOT beams for each MOT were obtained.

For the upper MOT, total power in the three MOT beams entering the chamber was ~26 mW (with ~17 mW in cooling part and ~9 mW in re-pumping part). The diameter of each MOT beam for upper MOT was ~10 mm. For the lower MOT, the total power in the three MOT beams entering the cell was ~27 mW (with ~18 mW in cooling part and ~9 mW in re-pumping part). The diameter of each MOT beam for lower MOT was ~7 mm. All the lasers were frequency stabilized and locked using saturated absorption spectroscopy (SAS). The cooling lasers were locked at ~12 MHz to the red of $5S_{1/2}$ F = 2→$5P_{3/2}$ F' = 3 transition of ^{87}Rb, whereas re-pumping laser was locked at peak of its $5S_{1/2}$ F = 1→$5P_{3/2}$ F' =2 transition. The required polarizations of the MOT beams were set using quarter-wave plates. The quadrupole coils (QC) for upper MOT generated the axial magnetic field gradient of ~12 G/cm at DC current of 3.1 A, and those for lower MOT generated the axial magnetic field gradient of ~10 G/cm at current of 2.8 A.

The push beam (PB) was a continuous wave (cw) Gaussian laser beam (~100-200 μW) and resonant to $5S_{1/2}$ F = 1→$5P_{3/2}$ F' =2 transition. It was focused to $1/e^2$ size ~100μm on the upper MOT position, which corresponds to an intensity of ~10^3 mW/cm^2 at the upper MOT and ~13 mW/cm^2 at the lower MOT position for a power of ~150μW.

In absence of the push beam, the upper MOT captures ~1.4×10^6 atoms whereas the lower MOT does not have any measurable number. After applying the push beam, due to the push beam acceleration (~1.1×10^5 m/s^2 at ~160μW), the atoms from the upper MOT are ejected in form of continuous flux, and are captured again in the lower MOT inside the glass cell. The number of atoms in the lower MOT varies with the push beam power, and was found to be maximum for a push beam power of ~160μW. This optimum power can be correlated to the trap depth of upper MOT and capture velocity of the lower MOT.

We have estimated the number of atoms in a MOT by fluorescence imaging technique using a digital CCD camera (PixelFly, PCO, Germany). From the fluorescence image of a MOT cloud, the number of atoms (N) can be obtained using the relation,

$$N = N_c \frac{8\pi\left[1+4\left(\frac{\Delta}{\Gamma}\right)^2+6\frac{I_0}{I_{sat}}\right]}{\Gamma\left(6\frac{I_0}{I_{sat}}\right)\eta\,\Omega\,t_{exp}}$$

where N_c is total number of counts in the image, t_{exp} is CCD exposure time, is quantum efficiency of CCD, I_{sat} is saturation intensity for atomic transition, I_0 is the total intensity of cooling beams in the MOT, Γ=2πx5.9 MHz is the ^{87}Rb natural line-width, Δ is detuning of cooling beam and Ω is solid angle for the collection of fluorescence from atoms on CCD. The number (N) obtained by this method was found comparable to that measured by collecting the fluorescence on a high sensitivity photodiode [5].

In our efforts to improve the number in the lower MOT, we found that a weakly focussed hollow laser beam propagating vertically upward from the lower MOT side to the upper MOT can enhance the number in the lower MOT. This enhancement depends upon the detuning of the hollow beam from $5S_{1/2}$ F = 2→$5P_{3/2}$ F' = 3 transition [6]. Fig.T.1.3 and Fig.T.1.4 show the observed enhancement results for number in lower MOT for different values of hollow beam detuning. The hollow beam was generated using a home-made metal axicon mirror as reported earlier [7].

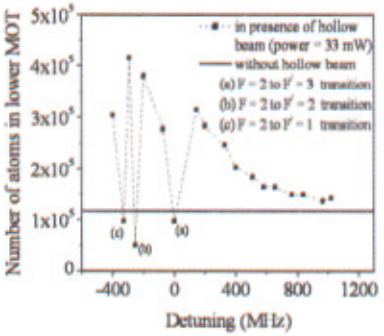

Fig.T.1.3. Measured variation of number of atoms in lower MOT with hollow beam detuning.

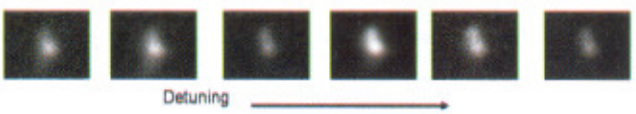

Fig.T.1.4. Images of lower MOT cloud for different hollow beam detuning values (some images showing enhancement in number).

The temperature of the atoms in MOT was measured by free expansion method which was to be ~200-400 μK in both the MOTs. It can be reduced further by applying molasses for some time on the atom cloud.

3.3. QUIC Magnetic Trap

For magnetic trapping and evaporative cooling of atoms trapped in lower MOT, we use a Quadrupole-Ioffe Configuration (QUIC) trap, first proposed and demonstrated by the Esslinger *et al* [8]. This is a simpler magnetic trap than time-averaged orbiting potential (TOP) trap and Ioffe-Pritchard (IP) trap, and operates at lower current than IP trap. A QUIC trap consists of two identical quadrupole coils and one Ioffe coil, which is conical in shape at one end. In a QUIC trap, as current in Ioffe coil is increased, the magnetic field

along the axis of the Ioffe coil (and hence the trapping potential) starts deforming and finally gives a nearly harmonic field distribution with nonzero off-set field to prevent Majorana spin flips.

The schematic of the QUIC trap, which we have developed for our BEC set-up, is shown in Fig.T.1.5. The coils dimensions were fixed by the simulations of magnetic field for the geometry appropriate to our set-up. The quadrupole coils have inner diameter of 34 mm, outer diameter of 69 mm and length of 37.5 mm. The Ioffe coil has a conical section of length 14 mm, minimum diameter of 6 mm (inner) and maximum diameter of 35 mm (outer). The straight section of the Ioffe coil has length of 21 mm with inner diameter of 6 mm and outer diameter of 35 mm. Each quadrupole coil has 184 turns and the Ioffe coil has 214 turns (160 in straight section 54 in conical section). The separation between the quadrupole coils was kept 50 mm. The distance between the end of the Ioffe coil and the symmetry axis of the quadrupole coils was kept 24 mm.

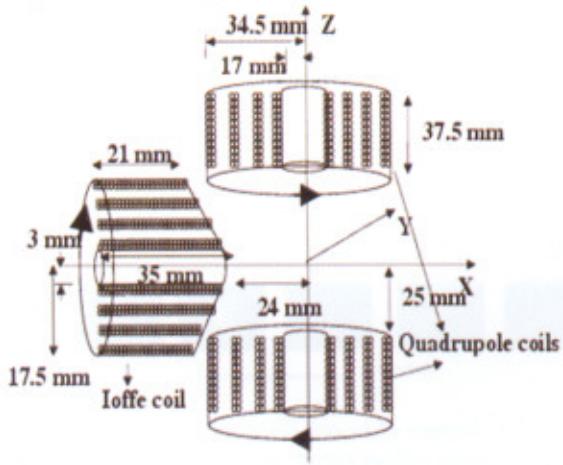

Fig.T.1.5. Schematic of arrangement of coils in QUIC trap for our set-up.

The coils were cooled by chilled water flowing in jackets surrounding them to remove the dissipated heat. The binding of coils was done in such a way that after every two layers, a spacer was positioned to create a gap for flow of water between the layers.

As expected, with increasing current in the Ioffe coil (I_{Ioffe}), the zero of the net magnetic field is shifted towards the Ioffe coil (Fig.T.1.6). The measured magnetic field of the trap for different values of I_{Ioffe} is as shown in Fig.T.1.6. At Ioffe coil current I_{Ioffe}= 29 A and quadrupole coil current I_q =23 A (Fig.T.1.6 b), we observed net field distribution becoming nearly harmonic with ~7 gauss as off-set field at the trap minimum [9]. The continuous curves in Fig.T.1.6 show the results of simulations, and experimental results were found in good agreement with it.

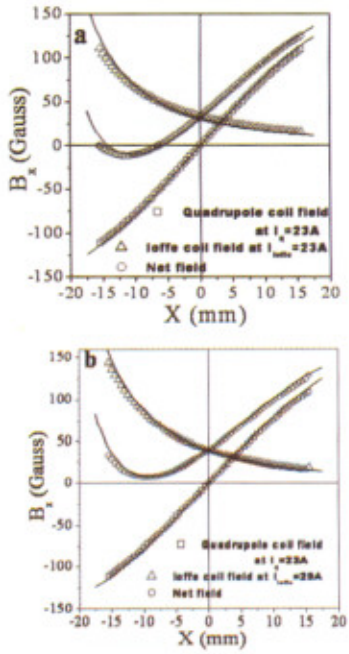

Fig.T.1.6. Variation of magnetic field with distance for a quadrupole coil current I_q =23 A and different values of Ioffe coil current I_{Ioffe}

3.4. Radio frequency (RF) evaporation system

The RF evaporation of atoms in a magnetic trap is a stimulated emission process which can be initiated by RF field of appropriate frequency such that photon energy ($h\nu_{rf}$) matches with the magnetic splitting between sublevels (as shown in Fig.T.1.7).

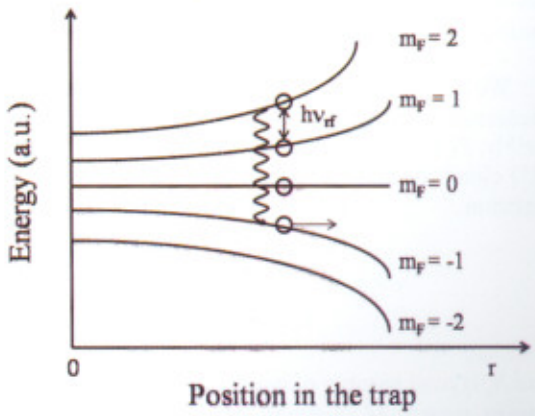

Fig.T.1.7. Schematic of the RF field stimulated transitions leading to ejection of an atom during RF-evaporation process.

To remove more energetic atoms from the trap, the frequency is swept in a calculated range from high to low in a specified time duration. In our RF evaporation system, we have planned to use a commercial RF synthesizer combined with a home-made amplifier system. The synthesizer can be controlled by LabVIEW on a PC to scan RF frequency in the desired range. The amplifier (developed at RF Systems & Control Division, RRCAT) amplifies the synthesizer signal upto ~2W. For our trap, the required scan range of RF is from ~14 MHz to 2 MHz, which is likely to get changed as the trap parameters and the initial temperature of atoms change.

3.5. Control system

Making Bose condensate in laser cooled atomic gases is a involved process which requires the operation of both the MOTs, the magnetic trap, the RF-evaporation, and detection and imaging, in a well controlled sequence of events. Step-wise, we have to perform laser cooling in the upper MOT, transfer the atoms to the lower-MOT, do optical pumping, do magnetic trapping in a QUIC trap, perform RF evaporative cooling, all in sequence, and then do detection and imaging to observe BEC. In order to accomplish the above events in the precise sequence, we need to activate and control several instruments within a short duration. The required precision in their activation time can be as short as few microseconds, which needs the control system to be accurate to that time scale. For this purpose, an electronic controller (18 output channels) compatible with LabVIEW and PC has been developed and programmed (by Laser Electronics Support Section, RRCAT) to provide appropriate switching pulses to activate different instruments and devices. Various devices controlled here include acousto-optic modulators for switching the MOT laser beams, power supplies for current in coils, RF synthesizer, CCD camera etc, to execute the sequence of events from MOT formation to RF-evaporation and imaging. The control system has been tested. Using this system, efforts to operate magnetic trap for atoms are in progress.

4. Conclusion

To conclude, we have developed a double-MOT set-up for BEC of ^{87}Rb atoms and made both the MOTs operational. We have gained expertise in characterization of the cold atoms, designed and tested a QUIC trap for magnetic trapping of the atoms, and got developed and tested control system and RF system. Presently we are in the process of loading atoms in the magnetic trap, a stage just before the RF-evaporation to form BEC.

We are very grateful to many colleagues at RRCAT for their continuous support and help in all this development. Specially, we would like to thank Mrs. L. Jain, Mrs. S. Tiwari, V. Bhanage, P. P. Deshpande, M. A. Ansari, H. R. Bundel and C. P. Navathe, all of Laser Electronics Support Section, RRCAT, for development of control system for the set-up, and M. Lad, P. R. Hannurkar and their colleagues at RF Systems & Control Division, RRCAT, for development of RF amplifier system. We are also thankful to C. Rajan and P. Kumar, LBAID, RRCAT, for development of high current switching circuits, S. Raja, LBAID, RRCAT, for fabrication of the tapered tube used in vacuum chamber, and H. S. Vora, LSED, for his help in CCD image processing. Finally, we thank Dr. S. C. Mehendale for a critical reading of the manuscript.

References:

1. M. H. Anderson, J. R. Ensher, M. R. Mathews, C. E. Wieman, E. A. Cornell, *Science* **269**, 198 (1995).
2. "Bose-Einstein condensation in dilute atomic gases", *Proc. International School of Physics* (Enrico Fermi course CXL), Edited by, M Inguscio, S. Stringari, and C. Wieman (IOS Press Amesterdam, 1999).
3. C. J. Myatt, N. R. Newbury, R. W. Ghrist, S. Loutzenhiser, and C. E. Wieman, *Opt. Lett.* **21**, 290 (1996).
4. W.D. Phillips and H. Metcalf, *Phys. Rev. Lett.* **48**, 596 (1992); T.E. Barret et al, *Phys. Rev. Lett.* **67**, 3483(1991).
5. V. B. Tiwari, S. R. Mishra, H. S. Rawat, S. Singh, S. P. Ram, S. C. Mehendale , *Pramana J. Phys.* **65**, 403 (2005).
6. S. R. Mishra, S. P. Ram, S. K. Tiwari, S. C. Mehendale, Proc. National Laser Symposium NLS-07 (Dec. 2007), Vadodara.
7. S. R. Mishra, S. K. Tiwari, S.P. Ram, S. C. Mehendale, *Opt. Eng.* **46**, 084002 (2007).
8. T. Esslinger, I. Bloch and T. W. Hänsch. *Phys. Rev. A* **58**, R2664 (1998).
9. S. R. Mishra, S. P. Ram, P. P. Dwivedi, S. K. Tiwari and S. C. Mehendale, Proc. Sixth DAE-BRNS National Laser Symposium NLS-06, (Dec 2006), Indore.